R. & M. No. 2823
(14,249)
(A.R.C. Technical Report)

MINISTRY OF SUPPLY

AERONAUTICAL RESEARCH COUNCIL
REPORTS AND MEMORANDA

Stress Concentrations at a Cut-out in a Swept Wing

By

E. H. MANSFIELD, M.A.

LONDON: HER MAJESTY'S STATIONERY OFFICE
1954
SIX SHILLINGS NET

Stress Concentrations at a Cut-out in a Swept Wing

By

E. H. MANSFIELD, M.A.

COMMUNICATED BY THE PRINCIPAL DIRECTOR OF SCIENTIFIC RESEARCH (AIR),
MINISTRY OF SUPPLY

*Reports and Memoranda No. 2823**

July, 1951

Summary.—The stress concentrations are determined for a panel, bounded by main load-carrying members and an oblique edge, such as might occur at a cut-out in a swept wing.

The solutions given are exact and cover the effects of a member along the oblique edge and of closely-spaced stringers attached to the panel.

1. *Introduction*.—The determination of the stress distribution in a panel bounded by two main members and an oblique edge between the members is complicated by difficulties in satisfying the boundary conditions along the oblique edge (R. & M. 2758[1]). The use of oblique co-ordinates (R. & M. 2754[2]) does not help since these still give rise to stress functions which are not orthogonal. It can be shown, however, that the stress distribution in the immediate vicinity of either main member and the oblique edge is independent of the stress distribution elsewhere. This means that such a localised stress distribution may be determined by ignoring the other main member and regarding the structure as an infinite wedge, bounded on the one side by one main member and on the other by the oblique edge. Furthermore, since the peak values of the shear stress in the actual panel occur where a main member and the oblique edge meet, the peak values of the shear stress can be determined exactly, and the distribution of stress near the peak values can be determined approximately*, if the structure is treated as an infinite wedge.

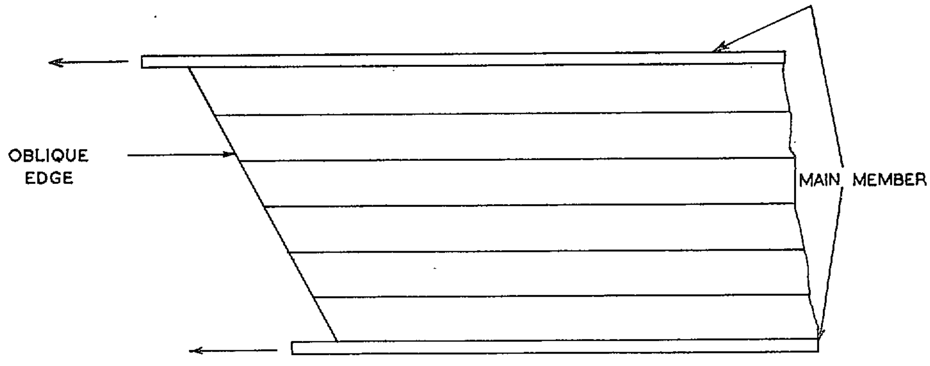

FIG. 1. Panel at cut-out in swept wing.

* R.A.E. Report Structures 114, received 1st October, 1951.

2. *Assumptions.*—In determining the stress distribution in the vicinity of the apex of the infinite wedge the following assumptions are made.

(*a*) stress-strain relations are linear

(*b*) buckling does not take place

(*c*) rivet flexibility is negligible

(*d*) the flexural rigidity of the main member and the oblique edge member, if any, is negligible

(*e*) if stringers (parallel to the main member) are present their stiffening effect may be adequately represented by assuming them to be spread out into an elastic sheet with equivalent directional properties.

Of these assumptions (*d*) is the most open to objection.

3. *Plain sheet.*—The analysis for the case when the sheet is not reinforced by stringers is simple and will be considered in detail. It is shown in Appendix I that the stress distribution in the immediate vicinity of the apex of the wedge is independent of the boundary conditions away from the apex; these boundary conditions may therefore be chosen to have the most convenient values to suit the analysis. They are chosen so that the stresses along the edges of the wedge are constant and equal to the values at the apex. This implies that the stress distribution in the wedge has a pattern which depends only on θ. *See* Fig. 2.

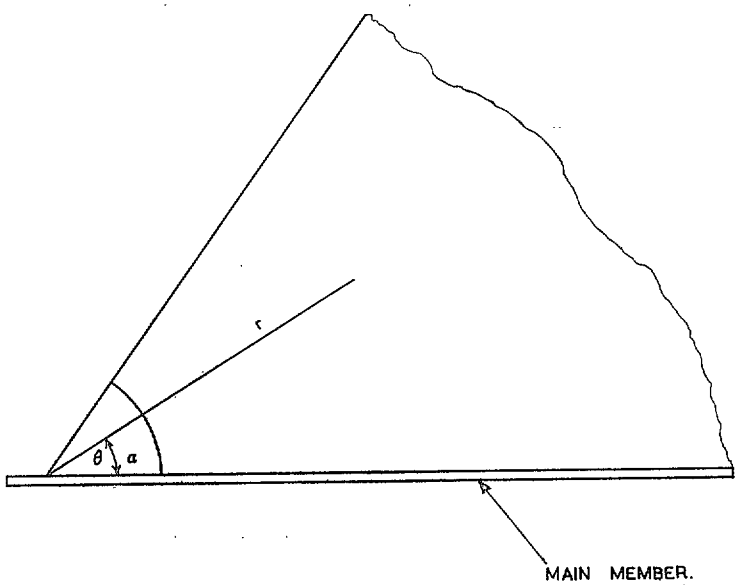

FIG. 2. The infinite wedge.

The most general form for the stress-function[3] which gives rise to such a stress pattern is

$$\phi = \tfrac{1}{2}r^2(a_1 - a_2 \sin 2\theta - a_3 \cos 2\theta + a_4\theta) \qquad \ldots \quad \ldots \quad \ldots \quad \ldots \quad (1)$$

where the a's are at present arbitrary. This function determines the following set of stresses,

$$\left.\begin{aligned} \sigma_r &= a_1 + a_2 \sin 2\theta + a_3 \cos 2\theta + a_4\theta \\ \sigma_\theta &= a_1 - a_2 \sin 2\theta - a_3 \cos 2\theta + a_4\theta \\ \tau_{r\theta} &= \phantom{a_1 +{}} a_2 \cos 2\theta - a_3 \sin 2\theta - \tfrac{1}{2}a_4 \end{aligned}\right\} \qquad \ldots \quad \ldots \quad \ldots \quad \ldots \quad (2)$$

* The values of $\partial\sigma/\partial r$ and $\partial\tau/\partial r$ at a corner in the actual panel are not determined by this analysis, but if the main members are tapered so as to have constant stress characteristics it can be shown that these derivatives are zero.

3.1. *Oblique Edge Free.*—The conditions along the free edge, $\theta = \alpha$, are

$$\sigma_\theta = \tau_{r\theta} = 0 \,,$$

and if $\hat{\sigma}_{r,m}$ is the direct stress in the main member the conditions at $\theta = 0$ are

$$\sigma_r - \nu\sigma_\theta = \hat{\sigma}_{r,m}$$

and by virtue of assumption (*d*)

$$\sigma_\theta = 0 \,.$$

These four conditions are sufficient to determine the four constants of equation (1) and thence the complete stress distribution, which has been plotted in Figs. 6 to 10 for values of α the wedge angle equal to 45 deg, 60 deg, 90 deg, 120 deg and 135 deg.

The peak value of the shear stress is given by

$$\tau_{r0,m} = \left[\frac{2\sin\alpha\,(\sin\alpha - \alpha\cos\alpha)}{\sin 2\alpha - 2\alpha\cos 2\alpha}\right]\hat{\sigma}_{r,m} \quad \ldots \quad (3)$$

and the direct stress along the free edge is

$$\sigma_{r,e} = \left[\frac{\sin 2\alpha - 2\alpha}{\sin 2\alpha - 2\alpha\cos 2\alpha}\right]\hat{\sigma}_{r,m} \,. \quad \ldots \quad (4)$$

The peak value of the shear stress has been plotted against α in Fig. 11. The factors in the brackets in expressions (3) and (4) above become infinite when $\alpha = 129$ deg and change their sense when $\alpha > 129$ deg. The reason for this becomes clearer if the problem is considered from the more direct approach of applying a known shear stress $\tau_{r0,m}$ to the wedge along $\theta = 0$ and then determining $\hat{\sigma}_{r,m}$ $(= \sigma_{r,m})$. The ratio $\hat{\sigma}_{r,m} : \tau_{r0,m}$ has been plotted in Fig. 12. With the shear stress acting in the sense shown in Fig. 12 $\hat{\sigma}_{r,m}$ is a tensile stress from 0 deg $< \theta <$ 129 deg and a compressive stress for $\theta >$ 129 deg, which might be expected as that part of the wedge for which $\theta >$ 90 deg tends to act in the nature of a buffer to the applied load.

In an actual construction the load is applied through a boom and equations (3) and (4) are no longer valid for $\alpha >$ 129 deg since they would then necessitate negative boom areas.

In practice it can be concluded that very high shear stresses will be developed when the wedge angle exceeds about 120 deg.

3.2. *Oblique Edge Supported.*—When there is a member along the oblique edge and the load is applied along the line of the main member, as in Fig. 3, there will be no load in the oblique edge member at the apex and the conditions along that edge in the simplified wedge structure will be

$$\sigma_\theta = 0 \,,$$
$$\hat{\sigma}_{r,e} = 0 \,.$$

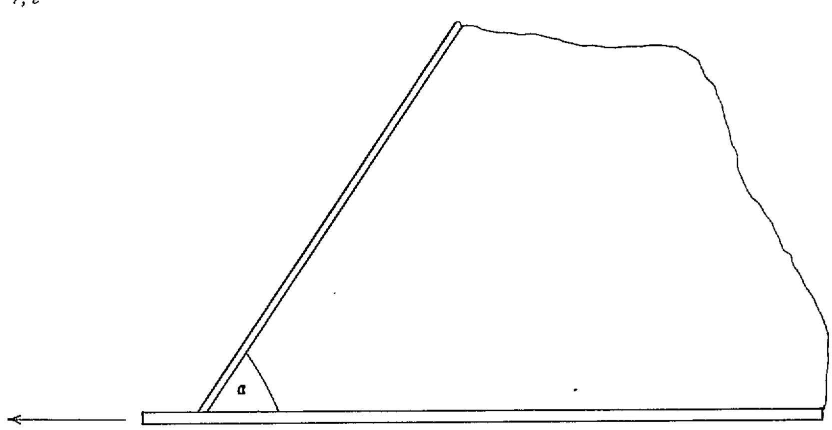

FIG. 3. Load applied along line of main member.

(61800) A*

The four constants of equation (1) are now determined and thence the complete stress distribution, which has been plotted in Figs. 13 to 17 for values of α the wedge angle equal to 45 deg, 60 deg, 90 deg, 120 deg and 135 deg.

The peak shear stresses occur at each edge of the wedge and are given by

$$\tau_{r0,m} = \left[\frac{1}{4\alpha} - \frac{\cot 2\alpha}{2}\right] \hat{\sigma}_{r,m} \quad \ldots \quad (5)$$

and

$$\tau_{r0,c} = \left[\frac{1}{4\alpha} - \frac{1}{2 \sin 2\alpha}\right] \hat{\sigma}_{r,m} \quad \ldots \quad (6)$$

The factors in the brackets of equations (5) and (6) become infinite when $\alpha = 90$ deg and change their sense when $\alpha > 90$ deg.

In an actual construction the load is applied through a boom and equations (5) and (6) are no longer valid for $a > 90$ deg since they would then necessitate negative boom areas. In practice flexural rigidity of the edge members will prevent very high shear stresses developing, but it can be concluded that high shear stresses are likely when the wedge angle exceeds about 80 deg.

3.2.1. *Oblique edge supported : loads in both edge members.*—If the applied load is at an angle β to the direction of the main member as in Fig. 4 below the stresses in the edge members are given by

$$\left.\begin{aligned} \hat{\sigma}_{r,m} &= \frac{P \sin (\alpha - \beta)}{A_m \sin \alpha} \\ \hat{\sigma}_{r,e} &= \frac{P \sin \beta}{A_e \sin \alpha} \end{aligned}\right\} \quad \ldots \quad (7)$$

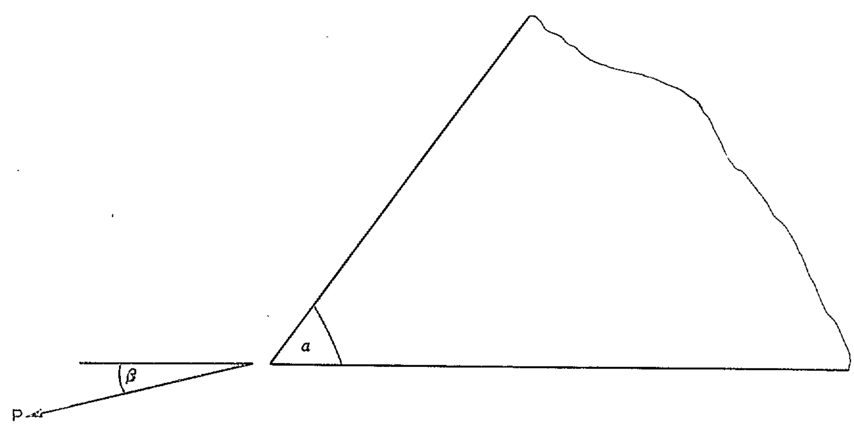

FIG. 4. Load applied at angle to main member.

The stress distribution is now obtained from a combination of those considered in section 3.2. In particular,

$$\tau_{r0,m} = \left[\frac{1}{4\alpha} - \frac{\cot 2\alpha}{2}\right] \hat{\sigma}_{r,m} + \left[\frac{1}{2 \sin 2\alpha} - \frac{1}{4\alpha}\right] \hat{\sigma}_{r,e} \quad \ldots \quad (8)$$

$$\tau_{r0,c} = \left[\frac{1}{4\alpha} - \frac{1}{2 \sin 2\alpha}\right] \hat{\sigma}_{r,m} + \left[\frac{\cot 2\alpha}{2} - \frac{1}{4\alpha}\right] \hat{\sigma}_{r,e} \quad \ldots \quad (9)$$

4. *Stringer-reinforced Sheet.*—The stress function corresponding to equation (1) differs only in that the last term $a_4\theta$ becomes $a_4H_0(\theta)$, where $H_0(\theta)$ has been derived in Appendix II. This stress function determined a set of stress resultants* $(\bar{\sigma}_r, \bar{\sigma}_0, \bar{\tau}_{r0})$ identical with that of equation (2)

* Stress resultants are here defined as (the resultant force in the stiffened sheet per unit length) $\div$ t. They therefore have the dimensions of a stress, and when there is no reinforcement the stress resultants are the actual stresses in the sheet.

except that the functions appropriate to a_4 become $H_1(\theta)$, $H_2(\theta)$, $H_3(\theta)$. These functions, which have been derived in Appendix II, have been tabulated (Tables 1 to 5) for different values of the stringer reinforcement parameter X.

4.1. *Oblique Edge Free.*—The peak value of the shear stress, adjacent to the main member, is given by

$$\tau_{r\theta,m} = \frac{(1 + X) \sin \alpha \, \{H_2(\alpha) \cos \alpha + H_3(\alpha) \sin a\}}{H_2(\alpha) \cos 2\alpha + H_3(\alpha) \sin 2\alpha} \hat{\sigma}_{r,m} . \qquad \ldots \qquad \ldots \qquad (10)$$

These values have been plotted against α in Fig. 11.

4.2. *Oblique Edge Supported.*—When there is a member along the oblique edge and the load is applied along the line of the main member, as in Fig. 3, the shear stress adjacent to the main member is given by

$$\tau_{r\theta,m} = \left[\frac{\begin{array}{l} H_1(\alpha) \sin^2 \alpha \, \{1 + X \sin^2 \alpha \, (1 + \nu)(1 + \cos^2 \alpha - \nu \sin^2 \alpha)\} \\ \quad - H_2(\alpha) \cos^2 \alpha \, \{1 + X \sin^4 \alpha \, (1 + \nu)^2\} \\ \quad + H_3(\alpha) \sin^2 \alpha \, \sin 2\alpha \, X(1 + \nu)(\cos^2 \alpha - \nu \sin^2 \alpha) \end{array}}{\begin{array}{l} H_1(\alpha)\{1 + X \sin^2 \alpha \, (1 + \nu)(1 + \cos^2 \alpha - \nu \sin^2 \alpha)\} \\ \quad + H_2(\alpha)\{1 + X(1 + \nu)[1 - \sin^2 \alpha \cos^2 \alpha \, (1 + \nu)]\} \\ \quad + H_3(\alpha) \sin 2\alpha \, X(1 + \nu)(\cos^2 \alpha - \nu \sin^2 \alpha) \end{array}} \right] \frac{(1 + X)\hat{\sigma}_{r,m}}{\sin 2\alpha} . \qquad (11)$$

5. *Range of Validity.*—The present analysis gives only the peak values of the stresses with no suggestion as to the rate at which these die away. Some indication of this rate may, however, be obtained from a consideration of Fig. 18. Fig. 18 shows contours of constant shear stress τ_{xy} in a rectangular panel with the booms tapered so as to be uniformly stressed. It will be seen that the 'θ-distribution' considered in this report has an approximate range of validity extending over regions within about $\frac{1}{3}$-panel width from each corner. If the booms are untapered the range of validity will be somewhat smaller. Further, the integral of the shear stress along each edge must equal the total load transferred to the sheet, so that in a swept panel bounded by untapered booms the greater shear stress will die away at a greater rate than the smaller shear stress. Thus we expect the range of validity of the θ-distributions to be increased at an acute angle and decreased at an obtuse angle.

6. *Conclusions.*—Exact solutions have been obtained for the stress concentrations which occur at a cut-out in a swept wing. The solutions include the effects of a member along the oblique edge and of closely spaced stringers attached to the panel. The analysis has been simplified by using the fact that the stress distribution in the immediate vicinity of either main member and the oblique edge is independent of the stress distribution elsewhere.

LIST OF SYMBOLS

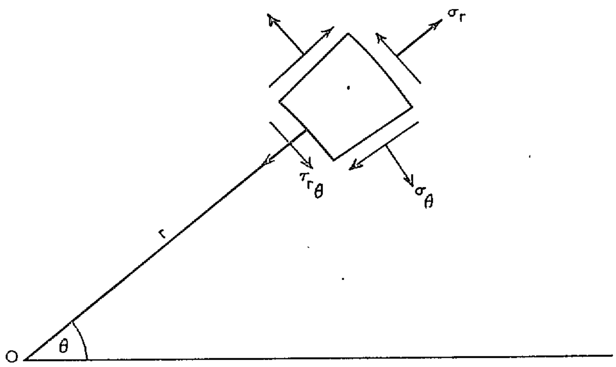

FIG. 5. Direction of positive stresses.

r, θ	Polar co-ordinates
ϕ	Stress function
a_1, a_2, a_3, a_4	Arbitrary constants
σ_r	Direct radial stress
σ_θ	Direct tangential stress
$\tau_{r\theta}$	Shear stress
$\hat{\sigma}_r$	Direct radial stress in tension member attached to sheet
α	Angle of wedge
β	Offset angle of applied load
A	Section area of member
t	Sheet thickness
X	Relative section area of stringer reinforcement
$=$	Stringer area $\div$ ($t \times$ stringer pitch)
$\bar{\sigma}_r, \bar{\sigma}_\theta, \bar{\tau}_{r\theta}$	Stress resultants for reinforced sheet
$H_0(\theta)$	Stress function for reinforced sheet
$H_1(\theta), H_2(\theta), H_3(\theta)$	Stress resultants appropriate to $H_0(\theta)$

Suffices $_m$ and $_e$ refer to the main member and edge member respectively ; *e.g.*,

$\hat{\sigma}_{r,m}$	Direct stress in main member
$\tau_{r\theta,m}$	Shear stress in sheet adjacent to main member
A_e	Section area of edge member

REFERENCES

No.	*Author*	*Title, etc.*
1	E. H. Mansfield	Elasticity of a sheet reinforced by stringers and skew ribs, with applications to swept wings. R. & M. 2758. December, 1949.
2	W. S. Hemp	On the application of oblique co-ordinates to problems of plane elasticity and swept-back wings. R. & M. 2754. January, 1950.
3	S. Timoshenko	*Theory of Elasticity.* p. 114. McGraw-Hill Book Company.

APPENDIX I

To show that the Stress Distribution in the Immediate Vicinity of the Apex of a Wedge is Independent of the Boundary Conditions away from the Apex

If we preclude the possibility of singularities at the apex the most general form for the stresses in the wedge (in plain sheet) can be expressed as[3]

$$\sigma_r = -2D_0\theta + \sum_{n=0}^{\infty} r^n\{(n+2)A_n \cos(n+2)\theta + (n-2)B_n \cos n\theta + (n+2)C_n \sin(n+2)\theta + (n-2)D_n \sin n\theta\}$$

$$\sigma_\theta = -2D_0\theta - \sum_{n=0}^{\infty} r^n(n+2)\{A_n \cos(n+2)\theta + B_n \cos n\theta + C_n \sin(n+2)\theta + D_n \sin n\theta\}$$

$$\tau_{r\theta} = +D_0 - \sum_{n=0}^{\infty} r^n\{(n+2)A_n \sin(n+2)\theta + nB_n \sin n\theta - (n+2)C_n \cos(n+2)\theta - nD_n \cos n\theta\}\,. \qquad (12)$$

The most general form for the boundary conditions expressed in terms of the stresses is

$$\left.\begin{aligned}
[\lambda_1\sigma_r + \lambda_2\sigma_\theta + \lambda_3\tau_{r\theta}]_m &= \sum_{n=0}^{\infty} K_n r^n \\
[\lambda_4\sigma_r + \lambda_5\sigma_\theta + \lambda_6\tau_{r\theta}]_m &= \sum_{n=0}^{\infty} L_n r^n \\
[\lambda_7\sigma_r + \lambda_8\sigma_\theta + \lambda_9\tau_{r\theta}]_c &= \sum_{n=0}^{\infty} M_n r^n \\
[\lambda_{10}\sigma_r + \lambda_{11}\sigma_\theta + \lambda_{12}\tau_{r\theta}]_c &= \sum_{n=0}^{\infty} N_n r^n
\end{aligned}\right\} \qquad (13)$$

where the λ's are constants.

Equating coefficients of powers of r in equations (12) and (13) gives sets of simultaneous equations from which A_n, B_n, C_n, D_n may be determined. In particular taking $n = 0$ shows that A_0, B_0, C_0, D_0 are functions of K_0, L_0, M_0, N_0, and are independent of the other K, L, M, N's. Now at the apex r is zero so that K_0, L_0, M_0, N_0 are the boundary values at the apex. It follows from equation (12) that the stress distribution in the immediate vicinity of the apex of a wedge is independent of the boundary conditions away from the apex.

APPENDIX II

Stress Functions for Stringer-reinforced Sheet

The sheet is reinforced by stringers of relative section area X in the Ox direction, *i.e.*, parallel to $\theta = 0$.

In Cartesian co-ordinates the stress-function (R. & M. 2758[1]) equation is

$$\left(k_1^2 \frac{\partial^2}{\partial x^2} + \frac{\partial^2}{\partial y^2}\right)\left(k_2^2 \frac{\partial^2}{\partial x^2} + \frac{\partial^2}{\partial y^2}\right) \phi = 0 \qquad \ldots \qquad (14)$$

where

$$\left.\begin{aligned} k_1^2 &= 1 + (1 + \nu)[X + \sqrt{(X + X^2)}] \\ k_2^2 &= 1 + (1 + \nu)[X - \sqrt{(X + X^2)}] \end{aligned}\right\} \qquad \ldots \qquad (15)$$

and ν is Poisson's ratio.

If we search for a solution of equation (14) in the form

$$\left.\begin{aligned} \phi &= x^2 F(y/x) \\ &= x^2 F(\lambda), \text{ say} \end{aligned}\right\} \qquad \ldots \qquad (16)$$

the equation for F reduces to

$$\frac{d}{d\lambda}\left[(k_1^2\lambda^2 + 1)(k_2^2\lambda^2 + 1)\frac{d^3F}{d\lambda^3}\right] = 0 \qquad \ldots \qquad (17)$$

so that

$$\frac{d^3F}{d\lambda^3} = \frac{\text{a constant}}{(k_1^2\lambda^2 + 1)(k_2^2\lambda^2 + 1)}$$

and

$$F = \int_0^\lambda \int_0^\lambda \int_0^\lambda (d\lambda)^3 \cdot \frac{\text{a constant}}{(k_1^2\lambda^2 + 1)(k_2^2\lambda^2 + 1)} + a + b\lambda + c\lambda^2 \qquad \ldots \qquad (18)$$

the three constants of integration corresponding to the three simple solutions of equation (14), namely $\phi = ax^2 + bxy + cy^2$.

The integral of equation (18) may be integrated to give

$$F \propto \left(\frac{k_1^2\lambda^2 - 1}{2k_1}\right)\tan^{-1} k_1\lambda - \left(\frac{k_2^2\lambda^2 - 1}{2k_2}\right)\tan^{-1} k_2\lambda - \frac{\lambda}{2}\log\left(\frac{k_1^2\lambda^2 + 1}{k_2^2\lambda^2 + 1}\right). \qquad \ldots \qquad (19)$$

The appropriate stress function in polar co-ordinates is therefore

$$\frac{r^2}{2}\left\{\left(\frac{k_1^2 \sin^2\theta - \cos^2\theta}{k_1}\right)\tan^{-1}(k_1 \tan\theta) - \left(\frac{k_2^2 \sin^2\theta - \cos^2\theta}{k_2}\right)\tan^{-1}(k_2 \tan\theta)\right.$$

$$\left. - \sin\theta\,\cos\theta\,\log\left(\frac{1 + k_1^2\tan^2\theta}{1 + k_2^2\tan^2\theta}\right)\right\} = \frac{r^2}{2} H_0(\theta), \text{ say}. \qquad \ldots \qquad (20)$$

The stresses are related to the stress function by the relations

$$\left.\begin{aligned}\bar{\sigma}_r &= \frac{1}{r}\frac{\partial\phi}{\partial r} + \frac{1}{r^2}\frac{\partial^2\phi}{\partial\theta^2},\\ \bar{\sigma}_\theta &= \frac{\partial^2\phi}{\partial r^2},\\ \bar{\tau}_{r\theta} &= -\frac{\partial}{\partial r}\left(\frac{1}{r}\frac{\partial\phi}{\partial\theta}\right)\end{aligned}\right\}, \quad \ldots \quad (21)$$

i.e.,

$$\left.\begin{aligned}\bar{\sigma}_r = &\left(\frac{k_1^2\cos^2\theta - \sin^2\theta}{k_1}\right)\tan^{-1}(k_1\tan\theta)\\ &-\left(\frac{k_2^2\cos^2\theta - \sin^2\theta}{k_2}\right)\tan^{-1}(k_2\tan\theta)\\ &+\frac{\sin 2\theta}{2}\log\left(\frac{1+k_1^2\tan^2\theta}{1+k_2^2\tan^2\theta}\right)\\ = &H_1(\theta), \text{ say,}\end{aligned}\right\} \quad \ldots \quad (22)$$

$$\left.\begin{aligned}\bar{\sigma}_\theta = &\left(\frac{k_1^2\sin^2\theta - \cos^2\theta}{k_1}\right)\tan^{-1}(k_1\tan\theta)\\ &-\left(\frac{k_2^2\sin^2\theta - \cos^2\theta}{k_2}\right)\tan^{-1}(k_2\tan\theta)\\ &-\frac{\sin 2\theta}{2}\log\left(\frac{1+k_1^2\tan^2\theta}{1+k_2^2\tan^2\theta}\right)\\ = &H_2(\theta), \text{ say,}\end{aligned}\right\} \quad \ldots \quad (23)$$

$$\left.\begin{aligned}\bar{\tau}_{r\theta} = &-\frac{\sin 2\theta}{2}\left\{\left(\frac{1+k_1^2}{k_1}\right)\tan^{-1}(k_1\tan\theta) - \left(\frac{1+k_2^2}{k_2}\right)\tan^{-1}(k_2\tan\theta)\right\}\\ &+\frac{\cos 2\theta}{2}\log\left(\frac{1+k_1^2\tan^2\theta}{1+k_2^2\tan^2\theta}\right)\\ = &H_3(\theta), \text{ say.}\end{aligned}\right\} \quad (24)$$

A complete set of stress resultants which are independent of r is therefore

$$\left.\begin{aligned}\bar{\sigma}_r &= a_1 + a_2\sin 2\theta + a_3\cos 2\theta + a_4H_1(\theta),\\ \bar{\sigma}_\theta &= a_1 - a_2\sin 2\theta - a_3\cos 2\theta + a_4H_2(\theta),\\ \bar{\tau}_{r\theta} &= \phantom{a_1 + {}} a_2\cos 2\theta - a_3\sin 2\theta + a_4H_3(\theta),\end{aligned}\right\} \quad \ldots \quad (25)$$

where the a's are arbitrary constants.

Tables of these H functions follow.

TABLE 1

H functions for $X = 0\cdot25$

θ (deg)	$H_1(\theta)$	$H_2(\theta)$	$H_3(\theta)$
0	0	0	0
5	0·12146	0·00031	—0·00530
10	0·23996	0·00246	—0·02100
15	0·35276	0·00821	—0·04648
20	0·45755	0·01920	—0·08075
25	0·55250	0·03683	—0·12251
30	0·63637	0·06230	—0·17020
35	0·70844	0·09649	—0·22211
40	0·76851	0·13997	—0·27639
45	0·81683	0·19301	—0·33114
50	0·85395	0·25550	—0·38466
55	0·88084	0·32709	—0·43507
60	0·89866	0·40710	—0·48080
65	0·90877	0·49457	—0·52042
70	0·91267	0·58833	—0·55273
75	0·91192	0·68703	—0·57675
80	0·90809	0·78914	—0·59179
85	0·90277	0·89305	—0·59742
90	0·89748	0·99712	—0·59348
95	0·89370	1·09967	—0·58012
100	0·89287	1·19909	—0·55771
105	0·89638	1·29386	—0·52693
110	0·90559	1·38259	—0·48868
115	0·92177	1·46407	—0·44409
120	0·94611	1·53732	—0·39451
125	0·97967	1·60158	—0·34144
130	1·02334	1·65639	—0·28654
135	1·07777	1·70158	—0·23150
140	1·14338	1·73732	—0·17826
145	1·22023	1·76402	—0·12847
150	1·30805	1·78247	—0·08391
155	1·44769	1·79371	—0·04618
160	1·51338	1·79907	—0·01671
165	1·62812	1·80009	+0·00334
170	1·74502	1·80395	+0·01149
175	1·87126	1·79616	+0·01200
180	1·99423	1·79495	0

TABLE 2

H functions for $X = 0 \cdot 5$

θ (deg)	$H_1(\theta)$	$H_2(\theta)$	$H_3(\theta)$
0	0	0	0
5	0·18787	0·00048	—0·00821
10	0·36946	0·00380	—0·03244
15	0·53930	0·01267	—0·07153
20	0·69314	0·02953	—0·12365
25	0·82822	0·05646	—0·18651
30	0·94309	0·09510	—0·25742
35	1·03744	0·14662	—0·33354
40	1·11180	0·21166	—0·41193
45	1·16735	0·29037	—0·48970
50	1·20580	0·38240	—0·56410
55	1·22921	0·48693	—0·63260
60	1·23991	0·60274	—0·69295
65	1·24042	0·72823	—0·74323
70	1·23331	0·86150	—0·78190
75	1·22115	1·00042	—0·80781
80	1·20639	1·14270	—0·82025
85	1·19133	1·28594	—0·81889
90	1·17809	1·42775	—0·80383
95	1·16865	1·56576	—0·77554
100	1·16485	1·69774	—0·73421
105	1·16848	1·82163	—0·68298
110	1·18127	1·93559	—0·62142
115	1·20494	2·03808	—0·55198
120	1·24110	2·12793	—0·47674
125	1·29124	2·20429	—0·39800
130	1·35669	2·26679	—0·31823
135	1·43849	2·31547	—0·24004
140	1·53740	2·35083	—0·16606
145	1·65379	2·37383	—0·09893
150	1·78757	2·38591	—0·04121
155	1·93810	2·38890	+0·00474
160	2·10395	2·38506	+0·03682
165	2·28275	2·37696	+0·05330
170	2·47098	2·36744	+0·05295
175	2·66384	2·35949	+0·03514
180	2·85550	2·35618	0

TABLE 3

H functions for $X = 0 \cdot 75$

θ (deg)	$H_1(\theta)$	$H_2(\theta)$	$H_3(\theta)$
0	0	0	0
5	0·24813	0·00063	−0·01085
10	0·48581	0·00502	−0·04278
15	0·70433	0·01669	−0·09400
20	0·89767	0·03879	−0·16176
25	1·06264	0·07388	−0·24272
30	1·19820	0·12405	−0·33303
35	1·30500	0·19049	−0·42885
40	1·38468	0·27384	−0·52626
45	1·43964	0·37406	−0·62152
50	1·47272	0·49047	−0·71113
55	1·48713	0·62178	−0·79198
60	1·48630	0·76625	−0·86134
65	1·47378	0·92165	−0·91699
70	1·45311	1·08544	−0·95722
75	1·42773	1·25482	−0·98086
80	1·40457	1·42682	−0·98728
85	1·37529	1·59843	−0·97638
90	1·35372	1·76666	−0·94855
95	1·33842	1·92861	−0·90467
100	1·33575	2·08159	−0·84605
105	1·33503	2·22317	−0·77441
110	1·35093	2·35126	−0·69179
115	1·38117	2·46416	−0·60066
120	1·42761	2·56060	−0·50372
125	1·49202	2·63982	−0·40394
130	1·57595	2·70162	−0·30447
135	1·68074	2·74631	−0·20858
140	1·80740	2·77483	−0·11960
145	1·95661	2·78865	−0·04082
150	2·12864	2·78985	+0·02459
155	2·32316	2·78107	+0·07361
160	2·53903	2·76526	+0·10367
165	2·77366	2·74607	+0·11247
170	3·02260	2·72733	+0·09845
175	3·27891	2·71303	+0·06085
180	3·53331	2·70744	0

TABLE 4

H functions for $X = 1 \cdot 0$

θ (deg)	$H_1(\theta)$	$H_2(\theta)$	$H_3(\theta)$
0	0	0	0
5	0·30583	0·00078	−0·01339
10	0·59615	0·00618	−0·05265
15	0·85869	0·02052	−0·11528
20	1·08595	0·04757	−0·19754
25	1·27478	0·09036	−0·29493
30	1·42520	0·15112	−0·40262
35	1·53912	0·23121	−0·51568
40	1·61954	0·33115	−0·62934
45	1·67010	0·45066	−0·73910
50	1·69480	0·58868	−0·84088
55	1·69792	0·74351	−0·93104
60	1·68390	0·91282	−1·00653
65	1·65721	1·09385	−1·06491
70	1·62226	1·28344	−1·10437
75	1·58326	1·47818	−1·12378
80	1·54407	1·67452	−1·12265
85	1·50810	1·86888	−1·10116
90	1·47833	2·05775	−1·06003
95	1·45737	2·23783	−1·00054
100	1·44755	2·40604	−0·92448
105	1·45103	2·55970	−0·83407
110	1·46997	2·69651	−0·73192
115	1·50644	2·81468	−0·62105
120	1·56248	2·91297	−0·50474
125	1·63999	2·99076	−0·38656
130	1·74067	3·04802	−0·27026
135	1·86599	3·08543	−0·15968
140	2·01716	3·10432	−0·05872
145	2·19515	3·10671	+0·02880
150	2·40060	3·09526	+0·09918
155	2·63375	3·07329	+0·14893
160	2·89400	3·04466	+0·17491
165	3·17919	3·01378	+0·17443
170	3·48442	2·98543	+0·14552
175	3·80088	2·96469	+0·08723
180	4·11551	2·95667	0

TABLE 5

H functions for $X = 1\cdot5$

θ (deg)	$H_1(\theta)$	$H_2(\theta)$	$H_3(\theta)$
0	0	0	0
5	0·41747	0·00107	—0·01830
10	0·80686	0·00843	—0·07167
15	1·14817	0·02788	—0·15589
20	1·43195	0·06430	—0·26502
25	1·65691	0·12145	—0·39227
30	1·82630	0·20188	—0·53071
35	1·94534	0·30696	—0·67360
40	2·01992	0·43690	—0·81464
45	2·05615	0·59088	—0·94808
50	2·06016	0·76711	—1·06880
55	2·03815	0·96296	—1·17243
60	1·99630	1·17515	—1·25540
65	1·94073	1·39982	—1·31499
70	1·87733	1·63270	—1·34934
75	1·81166	1·86930	—1·35751
80	1·74872	2·10503	—1·33939
85	1·69284	2·33535	—1·29568
90	1·64769	2·55590	—1·22784
95	1·61633	2·76266	—1·13797
100	1·60142	2·95200	—1·02876
105	1·60538	3·12083	—0·90340
110	1·63052	3·26662	—0·76555
115	1·67907	3·38756	—0·61925
120	1·75318	3·48254	—0·46886
125	1·85481	3·55125	—0·31898
130	1·98571	3·59423	—0·17438
135	2·14744	3·61271	—0·03986
140	2·34138	3·60898	+0·07978
145	2·56888	3·58600	+0·17984
150	2·83139	3·54760	+0·25583
155	3·13047	3·49835	+0·30346
160	3·46738	3·44355	+0·31877
165	3·84196	3·38917	+0·29822
170	4·25017	3·34171	+0·23896
175	4·68054	3·30810	+0·13941
180	5·11181	3·29537	0

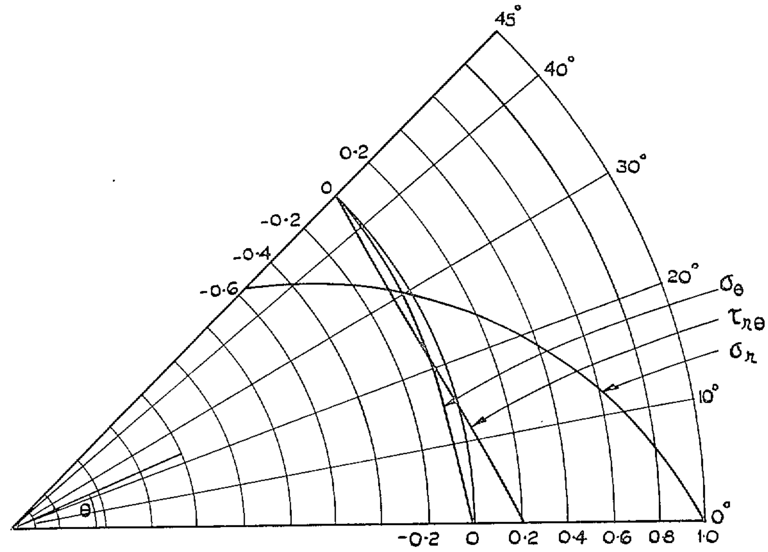

FIG. 6. Stress distribution in the neighbourhood of a 45-deg corner (constant-stress edge member along $\theta = 0$ deg; free edge along $\theta = 45$ deg).

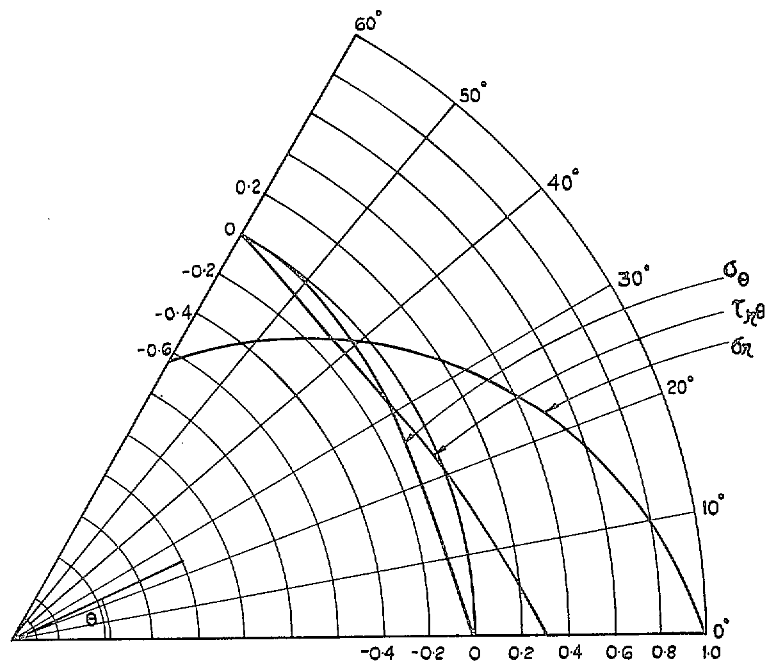

FIG. 7. Stress distribution in the neighbourhood of a 60-deg corner (constant-stress edge member along $\theta = 0$ deg; free edge along $\theta = 60$ deg).

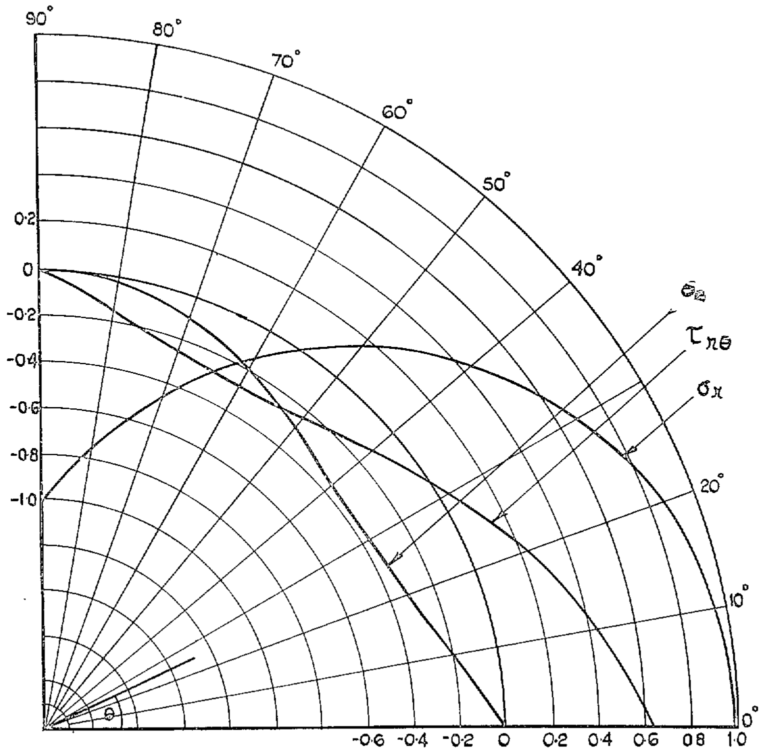

FIG. 8. Stress distribution in the neighbourhood of a 90-deg corner (constant-stress edge member along $\theta = 0$ deg; free edge along $\theta = 90$ deg).

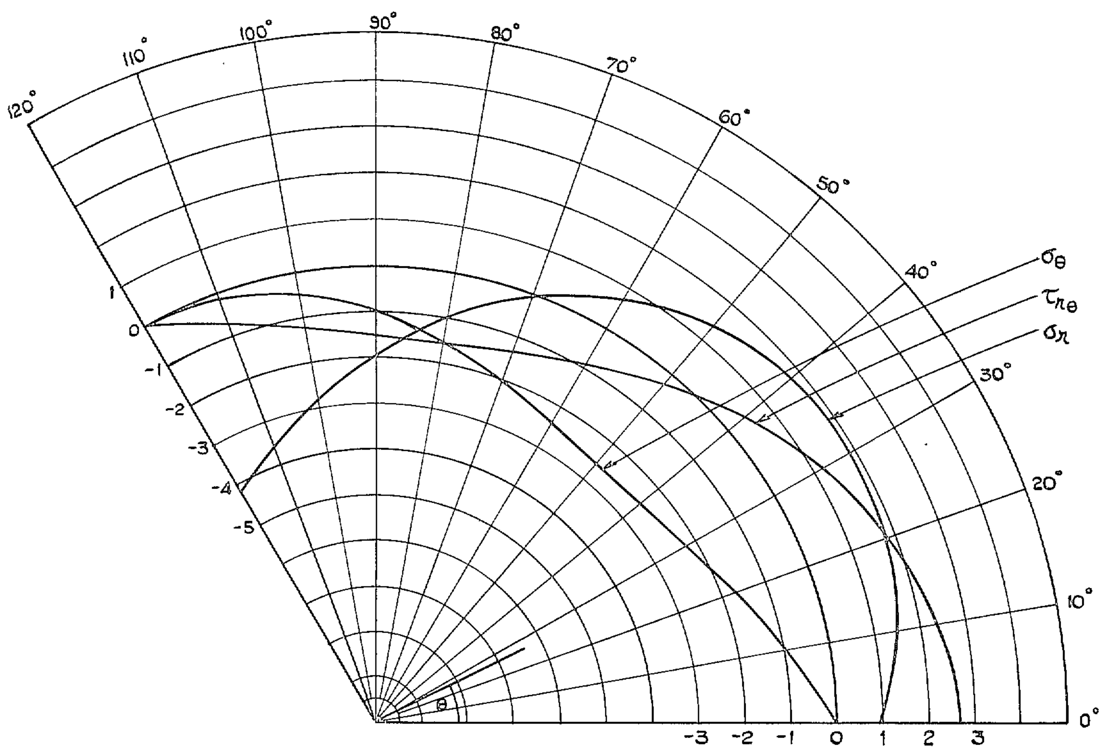

FIG. 9. Stress distribution in the neighbourhood of a 120-deg corner (constant-stress edge member along $\theta = 0$ deg; free edge along $\theta = 120$ deg).

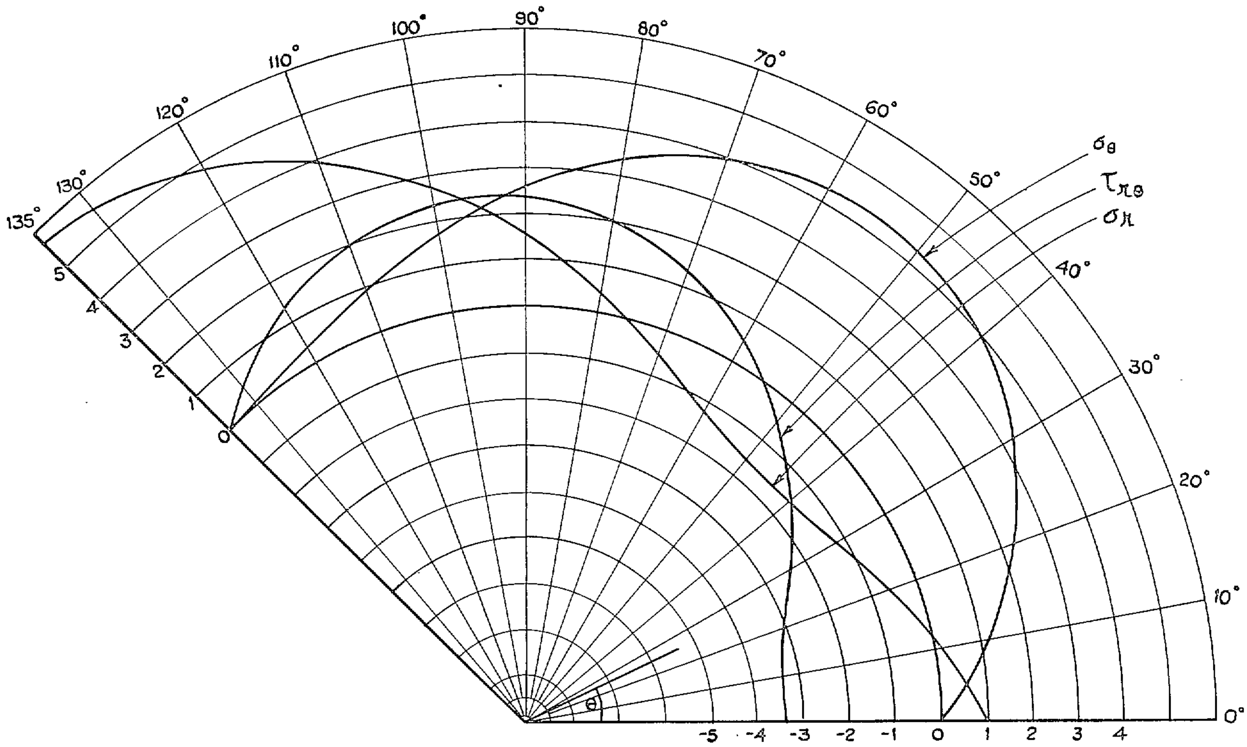

FIG. 10. Stress distribution in the neighbourhood of a 135-deg corner (constant-stress edge member along $\theta = 0$ deg; free edge along $\theta = 135$ deg).

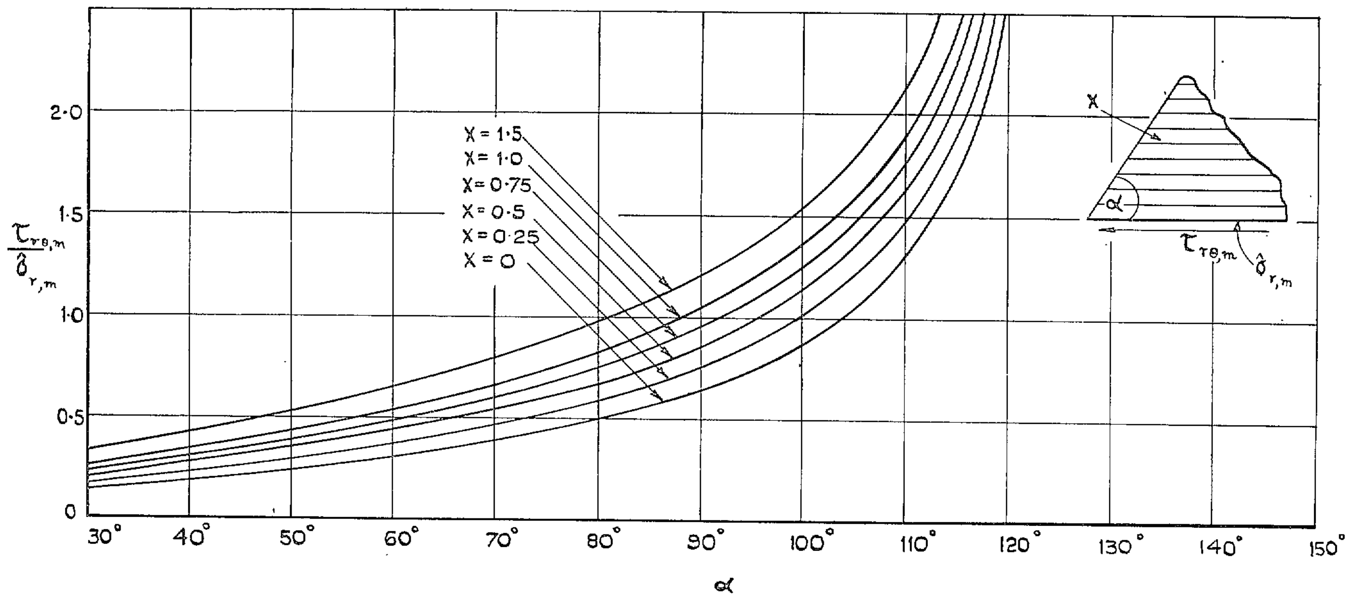

FIG. 11. Variation of $\tau_{r\theta,m}/\hat{\sigma}_{r,m}$ with α and X.

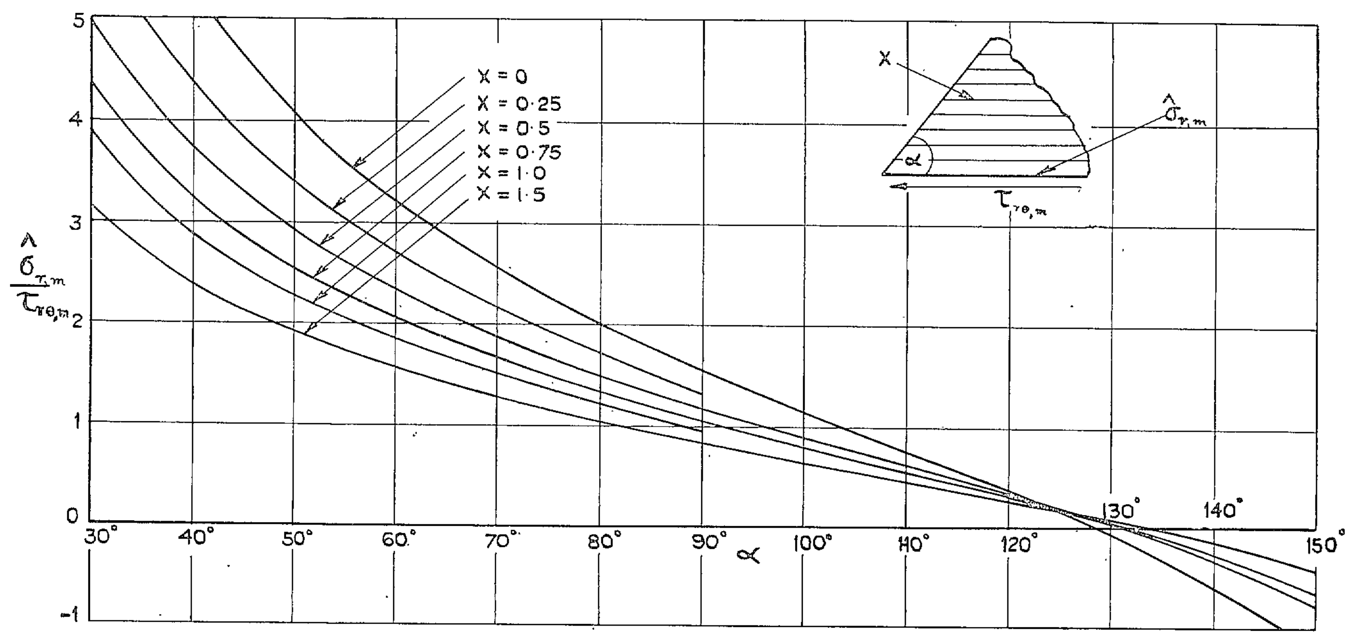

FIG. 12. Variation of $\hat{\sigma}_{r,m}/\tau_{r\theta,m}$ with α and X.

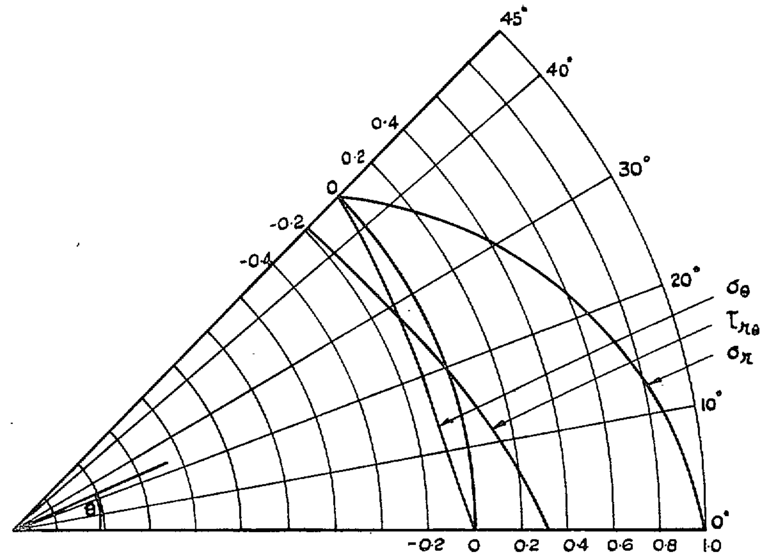

FIG. 13. Stress distribution in the neighbourhood of a 45-deg corner (constant-stress edge member along $\theta = 0$ deg; stiff edge member along $\theta = 45$ deg).

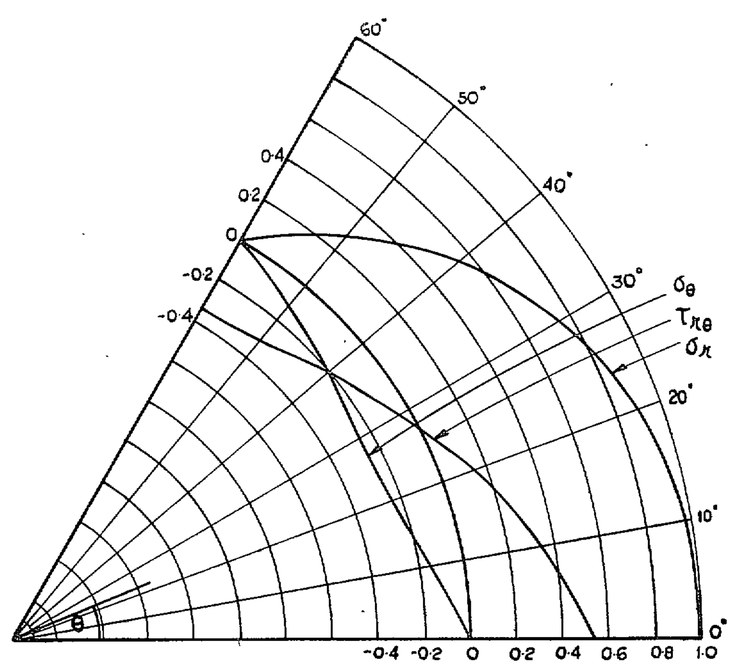

FIG. 14. Stress distribution in the neighbourhood of a 60-deg corner (constant-stress edge member along $\theta = 0$ deg; stiff edge member along $\theta = 60$ deg).

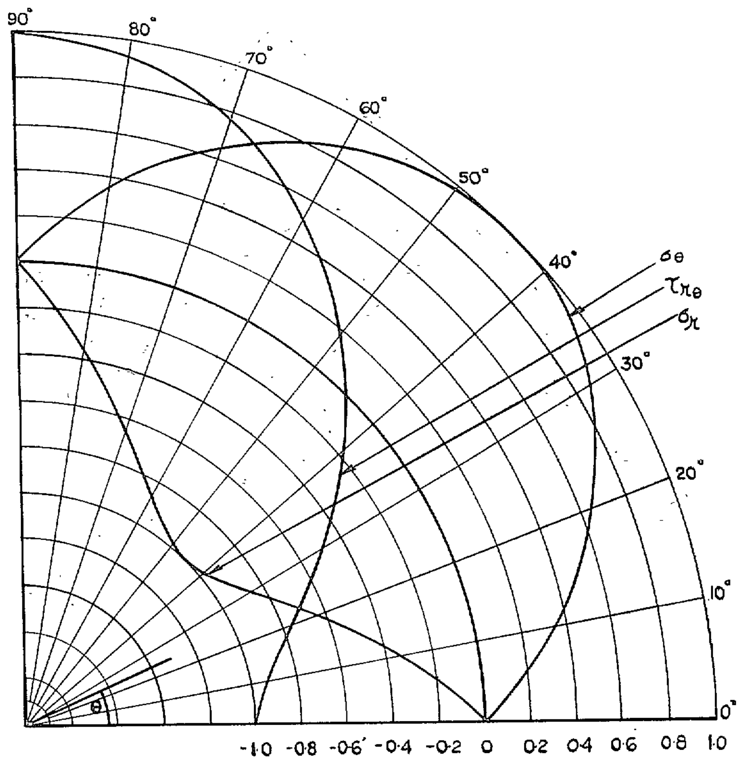

FIG. 15. Stress distribution in the neighbourhood of a 90-deg corner (unit shear applied along edge $\theta = 0$ deg; stiff edge member along $\theta = 90$ deg).

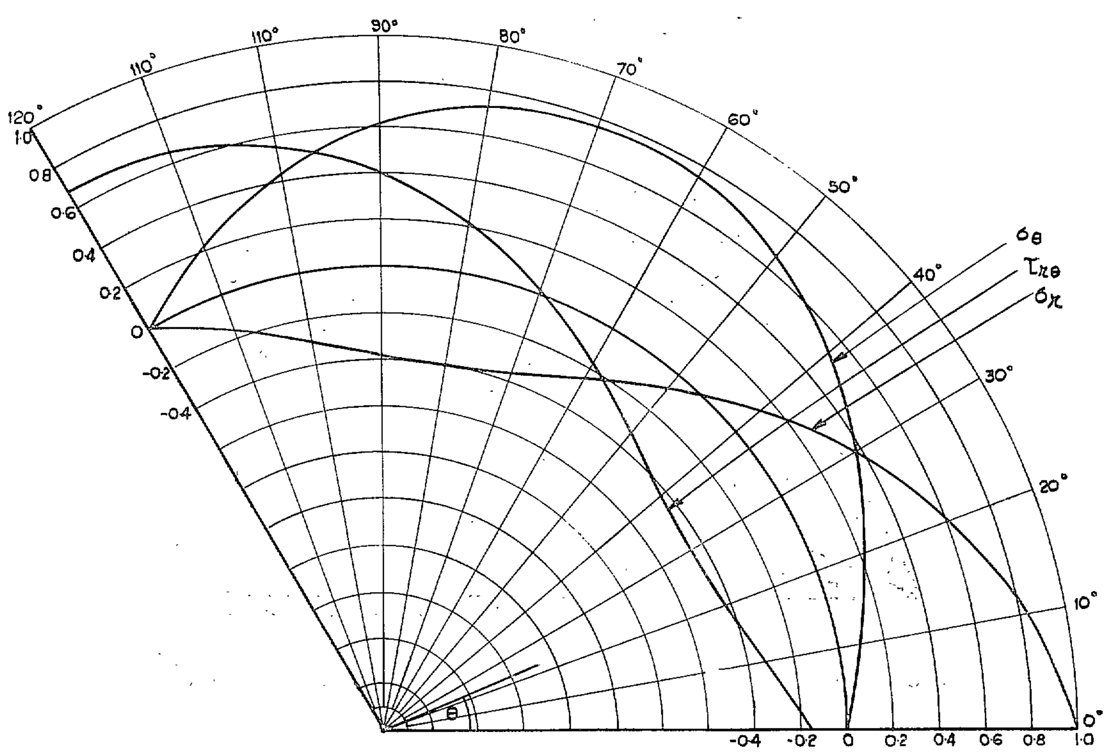

FIG. 16. Stress distribution in the neighbourhood of a 120-deg corner (constant-stress edge member along $\theta = 0$ deg; stiff edge member along $\theta = 120$ deg).

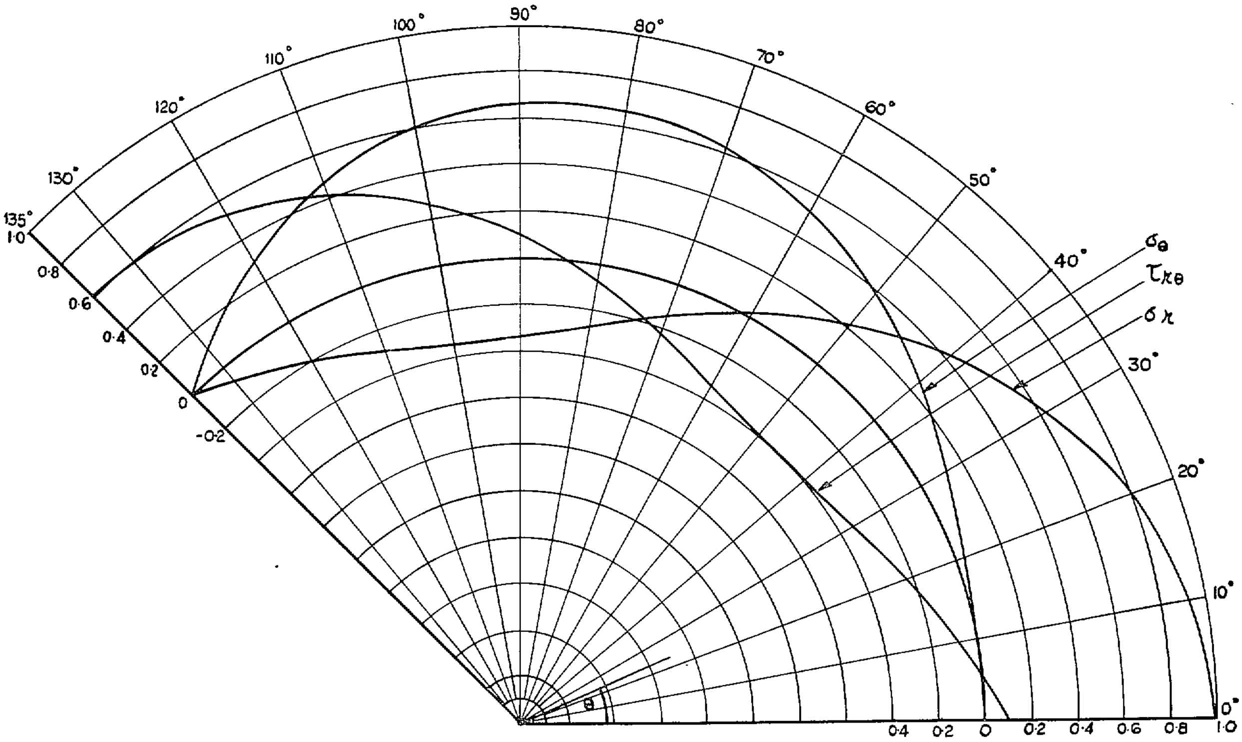

FIG. 17. Stress distribution in the neighbourhood of a 135-deg corner (constant-stress edge member along $\theta = 0$ deg; stiff edge member along $\theta = 135$ deg).

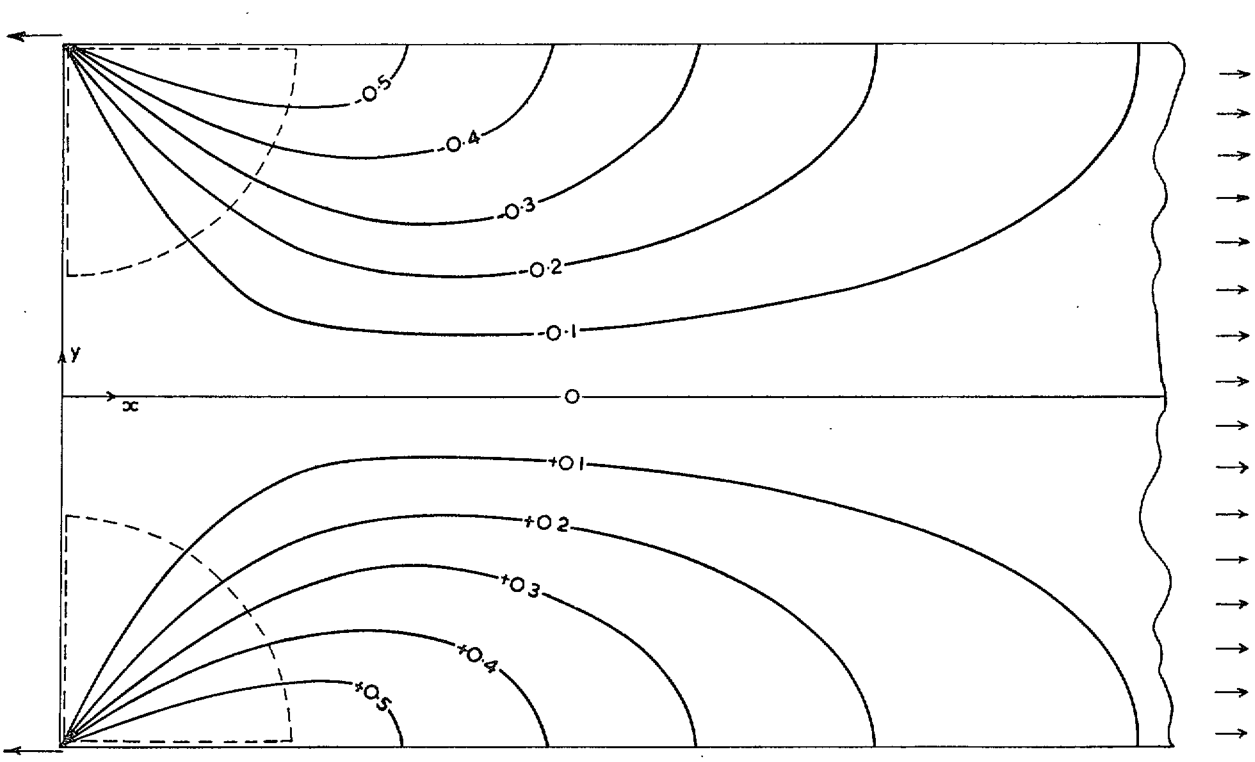

FIG. 18. Contours of constant $\tau_{xy}/\hat{\sigma}_{x,m}$ for a rectangular panel, showing the approximate range of validity of the θ-distributions.

(61800) Wt. 17/680 K.9 9/54 Hw. PRINTED IN GREAT BRITAIN

Publications of the Aeronautical Research Council

ANNUAL TECHNICAL REPORTS OF THE AERONAUTICAL RESEARCH COUNCIL (BOUND VOLUMES)

1936 Vol. I. Aerodynamics General, Performance, Airscrews, Flutter and Spinning. 40s. (41s. 1d.)
Vol. II. Stability and Control, Structures, Seaplanes, Engines, etc. 50s. (51s. 1d.)

1937 Vol. I. Aerodynamics General, Performance, Airscrews, Flutter and Spinning. 40s. (41s. 1d.)
Vol. II. Stability and Control, Structures, Seaplanes, Engines, etc. 60s. (61s. 1d.)

1938 Vol. I. Aerodynamics General, Performance, Airscrews. 50s. (51s. 1d.)
Vol. II. Stability and Control, Flutter, Structures, Seaplanes, Wind Tunnels, Materials. 30s. (31s. 1d.)

1939 Vol. I. Aerodynamics General, Performance, Airscrews, Engines. 50s. (51s. 1d.)
Vol. II. Stability and Control, Flutter and Vibration, Instruments, Structures, Seaplanes, etc. 63s. (64s. 2d.)

1940 Aero and Hydrodynamics, Aerofoils, Airscrews, Engines, Flutter, Icing, Stability and Control, Structures, and a miscellaneous section. 50s. (51s. 1d.)

1941 Aero and Hydrodynamics, Aerofoils, Airscrews, Engines, Flutter, Stability and Control, Structures. 63s. (64s. 2d.)

1942 Vol. I. Aero and Hydrodynamics, Aerofoils, Airscrews, Engines. 75s. (76s. 3d.)
Vol. II. Noise, Parachutes, Stability and Control, Structures, Vibration, Wind Tunnels. 47s. 6d. (48s. 7d.)

1943 Vol. I. Aerodynamics, Aerofoils, Airscrews. 80s. (81s. 4d.)
Vol. II. Engines, Flutter, Materials, Parachutes, Performance, Stability and Control, Structures. 90s. (91s. 6d.)

1944 Vol. I. Aero and Hydrodynamics, Aerofoils, Aircraft, Airscrews, Controls. 84s. (85s. 8d.)
Vol. II. Flutter and Vibration, Materials, Miscellaneous, Navigation, Parachutes, Performance, Plates and Panels, Stability, Structures, Test Equipment, Wind Tunnels. 84s. (85s. 8d.)

Annual Reports of the Aeronautical Research Council—

1933–34	1s. 6d. (1s. 8d.)	1937	2s. (2s. 2d.)
1934–35	1s. 6d. (1s. 8d.)	1938	1s. 6d. (1s. 8d.)
April 1, 1935 to Dec. 31, 1936	4s. (4s. 4d.)	1939–48	3s. (3s. 2d.)

Index to all Reports and Memoranda published in the Annual Technical Reports, and separately—

April, 1950 - - - - R. & M. No. 2600. 2s. 6d. (2s. 7½d.)

Author Index to all Reports and Memoranda of the Aeronautical Research Council—

1909–1949. R. & M. No. 2570. 15s. (15s. 3d.)

Indexes to the Technical Reports of the Aeronautical Research Council—

December 1, 1936 — June 30, 1939.	R. & M. No. 1850.	1s. 3d. (1s. 4½d.)
July 1, 1939 — June 30, 1945.	R. & M. No. 1950.	1s. (1s. 1½d.)
July 1, 1945 — June 30, 1946.	R. & M. No. 2050.	1s. (1s. 1½d.)
July 1, 1946 — December 31, 1946.	R. & M. No. 2150.	1s. 3d. (1s. 4½d.)
January 1, 1947 — June 30, 1947.	R. & M. No. 2250.	1s. 3d. (1s. 4½d.)
July, 1951.	R. & M. No. 2350.	1s. 9d. (1s. 10½d.)

Prices in brackets include postage.

Obtainable from

HER MAJESTY'S STATIONERY OFFICE

York House, Kingsway, London, W.C.2; 423 Oxford Street, London, W.1 (Post Orders: P.O. Box 569, London, S.E.1); 13a Castle Street, Edinburgh 2; 39, King Street, Manchester 2; 2 Edmund Street, Birmingham 3; 1 St. Andrew's Crescent, Cardiff; Tower Lane, Bristol 1; 80 Chichester Street, Belfast, or through any bookseller

S.O. Code No. 23-2823